

ADAMS Generic Engine: A Tribo-Elastodynamic Analysis Tool

A. Boysal *BSc, MSc* and H. Rahnejat *BSc, MSc, PhD, DIC, CEng, MIMechE, FCyS*

Department of Mechanical and Manufacturing Engineering, University of Bradford, Bradford,
West Yorkshire, BD7 1DP, UK

ABSTRACT

This paper presents a five degrees of freedom ADAMS multi-body dynamics model of a single cylinder internal combustion engine. The aim of the reported research project is to create a generic engine model which is parameterised to allow a design evaluation process. The engine model is customised in order to enable rapid model building. The model comprises of all rigid body inertial members, support bearings, the joints and joint primitives, couplers and connections between the various engine components, as well as means of vibration damping..

The engine model facilitates the monitoring of torsional vibrations of the crankshaft, as well as infinitesimal lateral vibrations of the crankshaft, support bearings and the flywheel by the virtue of appropriate selection of constraint functions. Non-linear lubricant reactions are included in the whirling of main shaft journal bearings, as well as in the contact of piston compression ring to the cylinder liner. The tribological contact models also provide instantaneous lubricant film thickness under hydrodynamic rolling/sliding and squeeze film conditions in journals, and a mixed regime of lubrication (rigid-isoviscous and elastohydrodynamics) in compression ring to cylinder liner. In addition to the above, eccentric rocking motion of the piston is allowed, causing secondary piston motions leading to the phenomenon of piston skirt to liner slapping action. A finite line elastic contact dynamic model is included for instantaneous contact loads carried at the rubbing surfaces of the piston skirt and the cylinder liner.

The combustion gas force and the corresponding piston friction forces are calculated by the model. Because the engine model provides simultaneous solution of small amplitude oscillations of lubricated contacts with large displacement dynamics of, for example, piston translation, the standard integrator parameters must be modified. These new parameters are included in the engine model.

1. INTRODUCTION

There are a multitude of causes that contribute to Noise, Vibration and Harshness (NVH) in reciprocating internal combustion engines. These include the application of periodic combustion forces in cylinders and the associated inertial forces of rotating and articulating members such as the crankshaft, the camshaft and the connecting rod. Eccentric rotation at journal bearing supports [1,2] and off-centre rotation of the flywheel as well as elastodynamic behaviour of the crankshaft account for other sources of noise and vibration. The combination of the latter two effects can lead to the further coupling phenomenon of flywheel “nodding”, caused by inducement of a gyroscopic moment.

Contact vibration problems also arise from meshing of gear teeth in timing gears [3,4], and noise and vibrations generated in the concentrated contact of other mating members such as the transient contact dynamics of cam/follower [5,6,7], as well as rolling element bearings to raceways in camshaft support bearings[8,9]. Other contributory factors include undesired secondary piston motions, resulting in “piston slap” (i.e. the rubbing of piston skirt against the cylinder liner) [10,11,12], and diminution of coherent lubrication between the piston compression ring and the cylinder wall [13,14].

The instantaneous radial component of the piston force is transmitted along the connecting rod and is applied to the crankpin. This force tends to pull the crankpin away and induces the instantaneous bearing support load. The tangential component of the piston force, on the other hand, is utilised in the rotation of the crankshaft. With every power stroke the piston transmitted force is initially increased in magnitude and is subsequently reduced at the end of the stroke. This action results in an imparted twist-untwist action of the crankshaft, causing torsional vibrations to occur. In a four stroke internal combustion engine, described in this paper, the fundamental frequency of the applied torque coincides with half speed of the crankshaft and its harmonics are at whole or half orders of the same speed. Indeed a translational imbalance is induced by the piston and connecting rod acceleration. Simple analytical calculations show that the spectral composition of this acceleration contains responses at the engine order and its even order harmonics. The extension of such an analysis indicates that in principle high vibratory induced torques may occur at all engine orders. In principle in multi-cylinder engines, cylinder firing phases can be so chosen as to eliminate the effect of odd or half order responses, providing that one can guard against any cylinder-to-cylinder combustion variation. However, the odd or half order responses cannot be entirely eliminated as simple analytic calculations indicate that in combined torsional and cylinder twist modes, the spectral content is dominated by these frequencies.

Whilst the investigation of all these multitude of engine NVH problems have been carried out in isolation and specific remedial actions can in most cases be carried out to minimise their effect, the generated vibration amplitudes can still be high enough in extreme cases to cause crankshaft or other engine component failures. It is true to state that in practice, a few of the critical speeds produce seriously high vibratory torque amplitudes [10], but long term contact wear and fatigue can and do play a significant role in the failure of engine components. Furthermore, the increasingly stringent regulations against noise and particulate emissions warrant a more detailed systematic approach in the design and design evaluation of the new generation of engines. This in itself points to a comprehensive strategy for the evaluation of interacting phenomena that govern engine efficiency and its NVH performance. This calls for an integrated and multi-disciplinary approach, incorporating large displacement non-linear rigid and elastodynamic analysis and infinitesimal contact vibrations. Although many numerical solutions for these problems have been undertaken in isolation, their combined effect has been rarely attempted and in particular not with the sufficient detail that can be utilised in practical applications. The dearth of such integrated methodology is largely responsible for the unexplained experimentally obtained high vibration amplitudes at unexpected rotational speeds. Such problems have been identified by many contributors, for instance by Draminsky [11]. Hestermann and Stone [12] have pointed out that the cause of unexpected multiples of engine speed is the variable inertial effects due to large displacement dynamics of rotating and articulating members or uneven cylinder firing. In multiple cylinder engines cylinder-to-cylinder combustion variation can account for some of these unexpected vibration contributions [13]. In general these secondary vibration peaks have been largely attributed to non-linear dynamic behaviour of system's overall inertial variation and the distributed system stiffness. This distributed system stiffness can for example be profoundly affected by hydrodynamic or elastohydrodynamic prevailing lubrication conditions in the contact of mating members[25].

There is, however a large body of literature on crankshaft torsional vibrations at different operating conditions. Zeischka et al. [15] highlight a multi-body elastodynamic model of the crankshaft and the engine block. In their model they have made use of finite element models of the crankshaft and the engine block which were subsequently imported to an overall 4-cylinder engine model, comprising of rigid body representation for the connecting rod and pistons. The hydrodynamic journal effects were implemented by an impedance method. The impedance charts provided journal forces as a function of parameters such as bearing dimensions, oil viscosity and eccentricity. Katano et al. [16] also developed a model for simulating crankshaft NVH characteristics. Their model included the resonant characteristics of the crankshaft, incorporating crankshaft flexibility and some oil film characteristics of the main journal bearings. They verified that there is a significant correlation between crankshaft behaviour and the rumbling noise and estimated the rumbling noise levels for different operating conditions.

Hestermann and Stone [17] developed a number of models to quantify the effect of variable inertia on a single cylinder engine in both time and frequency domains. Their work shows that the reciprocating

engines have the potential to exhibit secondary critical speeds due to the frequency intermodulation between the engine speed, the natural frequency orders and the forcing frequency orders. Song et al. [18] analysed the coupled crankshaft vibration. The coupling effect generates high amplitudes of vibrations when the natural frequencies of the torsional and the axial vibrations are equal to one another or when the axial vibration frequency is double that of the torsional mode. They investigated the torsional-axial interactions to clarify some unexpected vibrations of crankshafts.

Lacy [19] highlights the torsional analysis of a 4-cylinder gasoline engine. In his model the crankshaft nodes representing the main bearings were connected to the main bearing housing by an oil film model, first reported by Kikuchi [20]. This oil film model describes the linear and the rotary stiffnesses and the damping of the oil film. The mean eccentricity of each bearing is calculated by a conventional bearing oil film analysis at the desired engine conditions.

Lacy [19] assumed that a journal eccentricity is constant, resulting in an axi-symmetric oil film constraint. This assumption would hold true at high speeds and under steady state conditions. However, transient conditions at all speeds lead to small perturbations which can be significant and, thus, a complete solution of journal bearing dynamics under rolling and squeeze film action together with large displacement dynamics of reciprocating members is desired. With the presence of a torsional damper at the front-end main bearing, torsional oscillations of the crankshaft will be different to those occurring at the flywheel end. Furthermore, the distributed inertial effect exacerbates the non-linear planar motion of the crankshaft at the rear main journal bearing (in the vicinity of the flywheel). These conditions can contribute to the gyroscopic whirl of the crankshaft at various rotational speeds. The model presented in this paper attempts to highlight the existence of this problem, even under rigid body dynamics of the crankshaft. For this purpose a simultaneous solution of the rigid body dynamics of all inertial components, hydrodynamics of journal bearing reactions under pure entraining motion and rigid body squeeze effect is undertaken together with the combustion piston gas force during the compression and expansion strokes in the cylinder.

The model also incorporates the secondary motion of the piston in a single cylinder engine, leading to rubbing/slapping of the piston skirt against the cylinder liner as well as squeeze film lubrication between the piston ring and the cylinder wall.

The model described in this paper is completely parameterised and customised in order to furnish a suitable “front-end” for non-expert interactions with the model. The development of this “tribo-multi-body dynamic” model has been carried out in great detail in ADAMS and by a multi-disciplinary research team at the University of Bradford in order to create a generic engine modelling tool of sufficient detail that can be exploited by practising engine designers in a virtual prototyping and scenario building environment.

2. THE ENGINE MODEL

A single cylinder internal combustion engine model, comprising of a piston, connecting rod, crankshaft, flywheel, timing gear, the torsional damper and the crankshaft main journal bearings, is presented in this paper. The ADAMS model is illustrated in Figure 1. Unlike the previously mentioned multi-body engine models in the literature, the crankshaft main journal bearings’ hydrodynamic action under rolling entraining motion and the squeeze film action of journal to bearing shell are modelled. The “big-end” and “small-end” bearings are represented by scalar constraint functions imposed by a cylindrical and a universal joint respectively. These constraint functions closely represent the articulation of the connecting rod without a further consideration of another journal bearing. However, in the next phase of development these bearings will be modelled in detail.

All rigid body inertial properties of the parts and stiffness/damping characteristics of the torsional damper are included in the model and are parameterised, thus enabling the user to change the information to suit a particular design. The flywheel to crankshaft connection is represented by appropriate scalar constraint functions in order to enable induced torsional and lateral vibrations to take place.

The timing gear is modelled as a coupling constraint function, where the camshaft to crankshaft rotational relation is defined as 1:-2. Further work on the elastohydrodynamic contact of meshing gear teeth is being carried out, but not reported in this paper. An elastomeric torsional damper is mounted on the front-end of the crankshaft and forms the hub to which the crankshaft pulley is attached. The stiffness and damping properties of the elastomer is modelled as a torsional bush using a linear function in the first instance.

2.1 Combustion Force

The cylinder pressure can be calculated through the application of the first law of thermodynamics to the trapped air-fuel mass mixture. The gas mixture is treated as ideal with given air properties. The rate of change of pressure is, therefore [21]:

$$\begin{aligned}\frac{dP}{dt} &= \frac{\gamma-1}{V} \cdot \frac{dQ}{dt_{heat}} - \frac{\gamma}{V} P \frac{dV}{dt} - \frac{\gamma-1}{V} \cdot \frac{dQ}{dT} \\ \frac{dQ}{dt_{heat}} &= h_c \cdot \frac{d(m\theta)}{dt} \\ \frac{dQ}{dt_{tran}} &= h_t A (T_g - T_w)\end{aligned}$$

The mass fraction of the fuel burned is calculated as a Wiebe function [22] and the instantaneous heat transfer coefficient can be estimated by Woschini's [23] correlation. The instantaneous piston force acts on the piston crown surface area and is obtained by the simultaneous solution of the above differential equations and the integration of the pressure distribution there. The resulting piston gas force is illustrated in Figure 2.

The piston friction force that acts between the piston compression ring and the cylinder wall is formulated in terms of the instantaneous cylinder pressure in each stroke of the piston. The value of this friction force is obtained with respect to the crankshaft angular velocity and the instantaneous location of the contacting area, given in terms of the piston translational velocity.

Under the start up conditions, the crankshaft must rotate fast enough in order to cater for an air-fuel mixture to enter the cylinder. For this purpose an initial torque must be applied over a short period of time. This starter motor torque is experimentally monitored and applied in the model as a step function in terms of the crankshaft angular velocity.

2.2 The Journal Bearing Model

The main crankshaft journal bearings are subjected to peak applied loads at intervals of every two revolutions of the crankshaft in this single cylinder 4-stroke engine. In the absence of the big-end and small-end journals (in this model) and the elasticity of the crankpin, these dynamic loads are entirely carried by the instantaneously generated hydrodynamic reaction in the main crankshaft journal bearings. The lubricant film thickness is then determined by the bearing pressure under the design clearance between the crank journal and the bearing shell. A typical clearance of the order of a thousandth of the journal radius is assumed in this analysis. The hydrodynamic reaction is also dependent on the bearing width to diameter ratio. This is taken as 0.6 for the purpose of this analysis. The eccentric rotation of the journal generates the hydrodynamic entraining action as well as the rigid body squeeze effect. Therefore, a solution of the Reynold's equation, including the effect of squeeze film action is required. This solution has been obtained for the case of a rigid bearing shell and included in the engine model. In its simplified form, the

hydrodynamic journal bearing reaction can be considered as the superimposed contributions of the entraining motion and the squeeze film action as:

$$W = \frac{12 \cdot \Pi^2 \cdot \varepsilon \cdot \mu \cdot N \cdot \left(\frac{R}{c}\right)^2 \cdot b \cdot (2R)}{(2 + \varepsilon^2) \cdot (1 - \varepsilon^2)^{1/2}} - \frac{12 \cdot \mu \cdot b \cdot c \cdot \left(\frac{d\varepsilon}{dt}\right)}{\left(\frac{c}{R}\right)^3 \cdot (1 - \varepsilon^2)^{3/2}}$$

2.3 The Piston Assembly

Piston, piston rings and cylinder bore represent a coupled system governed by the interaction of the gas and the inertial forces as well as by the hydrodynamic film reactions. The dynamics of this coupled system strongly affects the performance of reciprocating IC engines. The lubrication characteristics affect the degree of wear of piston, piston-ring and cylinder liner which in turn determines the quality of the gas sealing between ring and the liner, that controls the blowby and oil consumption. Both of these factors are very critical in increasing the engine life and efficiency.

2.3.1 Piston Slap

Piston slap has been a serious concern among many engineers and manufacturers of diesel engines. It is because piston slap is not only one of major sources of noise, but also a source of deterioration of engine performance.

The basic mechanism of its occurrence is quite clear but the phenomenon is extremely complicated because of the involvement of many influencing factors. Basically, piston in a reciprocating engine undergoes small oscillatory motions in the cylinder bore as a result of the time varying gas and inertial forces acting on it. The piston position, sliding velocity and acceleration are functions of crank angle. It can be observed that in a plane normal to the wrist-pin axis there is an imbalance of forces and moments acting on the piston (see Figure 3). As a result, the piston executes small translations and rotations within the confinement of the cylinder clearance.

This movement within the clearance is simulated numerically by generating exact governing equations, which are derived from the dynamics of the system of two rigid bodies having the required degrees of freedom. The wrist-pin offset is included in the analysis indirectly by the parameterised shift of the centre of gravity of the piston from the centre line. This representation allows analysis to be carried out for different wrist-pin offsets.

The reaction forces generated due to tilt are modelled using Petrenko's equation given below:

$$W = \left(\frac{K_c^2 \cdot e}{\lambda^3} \right)^{1/2} \cdot \delta^{3/2}$$

where K_c is the effective modulus of elasticity calculated as:

$$K_c = \frac{8}{3} \cdot \frac{E_p \cdot E_c}{E_p \cdot (1 - \nu_p^2) + E_c \cdot (1 - \nu_c^2)}$$

The design angle, ψ , is calculated as:

$$\psi = \arccos \left\{ \frac{e}{4} \cdot \sqrt{\left(\frac{1}{R_{x1}} - \frac{1}{R_{x2}} \right)^2 + \left(\frac{1}{R_{y1}} - \frac{1}{R_{y2}} \right)^2 + 2 \cdot \left(\frac{1}{R_{x1}} - \frac{1}{R_{x2}} \right) \cdot \left(\frac{1}{R_{y1}} - \frac{1}{R_{y2}} \right) \cdot \cos(2 \cdot \phi)} \right\}$$

where e and radii are defined as:

$$e = \frac{4}{\left(\frac{1}{R_{x1}} + \frac{1}{R_{x2}} + \frac{1}{R_{y1}} + \frac{1}{R_{y2}} \right)}$$

R_{x1} = radius of the piston in yz-plane

R_{x2} = radius of the cylinder liner in yz-plane (-ive)

R_{y1} = radius of the piston in xz-plane

R_{y2} = radius of the cylinder liner in xz-plane (-ive)

ϕ = contact angle

2.3.2 Ring Lubrication Model

Piston rings perform the dual function of controlling the leakage of gases past the piston and the spread of the oil up the cylinder liner towards the combustion chamber. They are loaded against the cylinder liner by a combination of elastic and gas pressure forces and to carry these contact loads, with a satisfactory wear life they must be separated from the cylinder liner by a film of oil. It has been indicated that approximately 25-50 per cent of the mechanical losses in an IC engine are due to friction between the piston rings and the cylinder wall. In order to improve the mechanical efficiency and life of engines many theoretical and experimental work have been carried out to predict the performance characteristics of piston rings.

In addition to the main sliding motion piston rings also experience lateral motions which arise from the piston's secondary motion and/or an unbalanced lateral fluid film force exerted on the ring. The relation between the secondary piston movement and ring lateral movement has been observed experimentally by Noda et al. [24].

The film reaction forces are defined as SFORCEs using the equations below [25,26]:

$$W = \frac{K'}{h^\alpha \cdot e^{\left(\frac{\beta}{h}\right)^h}} \quad (\text{EHL})$$

$$K' = (1150)^{27} \cdot G^{*10.962} \cdot u^{*23.139} \cdot \frac{R^{29}}{E_R}$$

$$E_R = \frac{1 - \gamma^2}{\pi \cdot E} \quad \text{and} \quad u^* = \frac{u \cdot \eta_0 \cdot E_R}{R}$$

$$W = \frac{5.6 \cdot b \cdot u \cdot \eta \cdot R}{h} - \frac{3 \cdot \pi \cdot b \cdot \eta \cdot R^{3/2} \cdot \dot{h}}{\sqrt{2} \cdot h^{3/2}} \quad (\text{isoviscous})$$

3. METHOD OF SOLUTION

The solution is performed in ADAMS using the Gstiff integrator. Unlike large displacement rigid body dynamics simulations the required order of error for convergence in the current model that include infinitesimal contact vibrations should be in the order of nanometers. Furthermore, the default maximum step size should be chosen in such a way as to capture high frequency oscillations encountered under elastohydrodynamic and elastodynamic contact conditions, particularly under transient conditions. Typically the maximum step size should be in the region of tenths of milliseconds.

4. NUMERICAL RESULTS

Figure 4 shows the generated hydrodynamic lubrication reaction in the crankshaft main journal bearing, situated at the flywheel end. It can be observed that under the initial transient conditions the bearing reaction follows the engine order frequency. Under the steady state conditions observed after 0.5 seconds the main contribution appears at the half engine order (in this case at 8 Hz, for the engine speed of 960rpm). This half order whirl is typical of journal bearing response as observed by many researchers and is referred to as nonsynchronous half speed whirl. This is also indicated by the spectral content in the Fast Fourier Transfer (FFT) plot in Figure 5. As expected a number of multiples of the engine order, in particular 1½ and 2nd order contributions are also significant. If the revolute joint constraint, initially imposed between the flywheel and the ground, is replaced by an at-point constraint, flywheel nodding would take place and result in an initial sharp increase in the magnitude of the lubricant reaction (see Figure 6). This sharp increase is due to the squeeze generated in the journal bearing during the transient analysis which is actuated by the unstable flywheel nodding (see Figure 7). The magnitude of the hydrodynamic force and the amplitude of oscillation for nodding of flywheel are both unacceptably high because an initial static analysis cannot be carried out in the presence of the applied combustion gas. This is analogous to a full vehicle suspension model being subjected to a non-linear dynamic analysis from a curb height position without a prior static analysis having been carried out. Nevertheless, engine NVH problems are not initial value problems and initial transient condition does not affect the steady state solution. During steady state, the peak to peak amplitude indicates an oscillation of 2-3 degrees which can result in a significant axial movement at the rim of the flywheel at both half and the first engine orders. It should be noted that the half engine order frequency is found to be often responsible for cable operated clutch in-cycle vibration problems [25].

Due to wrist-pin offset secondary piston motion occur resulting in tilting of the piston during its reciprocating motion. Figure 8 shows piston tilt angle oscillations of the piston for a small 1 micron offset. Impractical situations a larger offset is expected. In fact the results obtained by Dennis et al. [27] indicate that piston motion is strongly affected by the location of wrist-pin and that the piston skirt friction is increased significantly if the wrist-pin is at an unfavourable position. Referring back to Figure 8, the sharp spikes in particular in the initial part of the analysis occur as the piston skirt slaps against the cylinder liner, introducing a significant contact force which tends to restore the piston motion to a pure translational action. Figure 9 depicts the variation of the slapping force. If the results of Figure 8 and 9 are taken in conjunction with one another it can be observed that the instances of high contact forces are related to rapid changes in the secondary motion of the piston. Every time the piston tilts at a lower frequency and is subjected to recurring slapping action. Although the amplitude of the slapping force is reduced in figure 8 longer time simulations indicate that large impact forces can recur. The secondary motion of the piston is largely of a continual transient nature and as such a spectral analysis of the tilting response indicates a considerable modulation effects which can be interpreted as contact induced carrier frequencies with

associated side bands. This is shown in Figure 10, where the two main carrier frequencies appear at 60 and 120 Hz. These frequencies may account for the so-called unexpected engine orders that have been reported by other authors for example by Draminsky [11].

The lubrication regime prevailing in the contact of piston compression ring to cylinder liner is modelled as a mixed regime; hydrodynamic, elastohydrodynamic and boundary lubrications. The boundary lubrication is a simplified model analogous to that of the piston skirt rubbing against the cylinder liner and under the simulation conditions it is observed that it does not contribute to the generated contact pressures under primary motion of the piston, it has been found by various authors, chiefly Dowson et al.[28] that the regime of lubrication remains mainly in the hydrodynamic (isoviscous elastic region). However, it has been shown by them and experimentally by Moore and Hamilton [29] that at the top dead centre the effect of EHL is particularly pronounced. With the secondary piston motions the contribution of EHL becomes dominant during the entire cycle. This is shown in Figures 11 and 12 for hydrodynamic and elastohydrodynamic lubricant reactions respectively. The oscillating nature of the reaction forces are due to the lateral movement of the piston ring. It can be observed that the hydrodynamic contribution is at least two orders of magnitude lower than the corresponding elastohydrodynamic value, indicating a small EHL film thickness under concentrated finite line conditions. This film thickness is shown in Figure 13. It indicates a steady state film of $4.89\text{ }\mu\text{m}$ thickness with a perturbation of approximately 1 nm is maintained for a $5\text{ }\mu\text{m}$ clearance. The R.M.S value of the combined surface roughness of the cylinder liner and the piston ring can be assumed in the region of $0.75\text{--}1\text{ }\mu\text{m}$ [29]. This means that if a lubricant film below this value is obtained, asperity interactions will take place leading to a larger coefficient of friction attainable with a coherent film. Under uninterrupted lubricated contacts one would expect a coefficient of friction in the region of $0.05\text{--}0.1$. However, there is various experimental findings indicating that coefficient of friction may be larger than this value pointing to metal to metal contact. This together with slapping of the piston skirt to the cylinder liner contributes significantly to the mechanical losses in internal combustion engines. Figure 14 shows the spectrum of oscillation of the elastohydrodynamic contact reaction between the ring and the cylinder liner. Two significant frequencies dominate the spectrum. The contribution at 16 Hz is at the engine order, indicating EHL contribution at top dead centre because at this location the system responds at a synchronous crankshaft speed. This phenomena has also been observed by Hamilton et al. [29] and the numerical discovery of this by the model is regarded as significant. At the top dead centre there is a significant depletion of lubricant film, observed experimentally, and in fact extrapolated lubricant film equations under EHL condition predict a zero film thickness owing to the momentary cessation of the entraining motion. However, a lubricant film is retained in reality due to elastic body squeeze film action which is also included in this reported model. The second dominant frequency is at twice engine order which is the only other significant frequency owing to piston acceleration. This in fact is a dominant frequency in all engine NVH problems. The absence of the half engine order (i.e. combustion force frequency) is because the EHL contact reaction is dominant at top dead centre, a point that is corroborated by the findings of Dowson et al. [28]. A corresponding FFT of the combustion force shows the half engine order, as expected, together with the other engine orders usually attributed to piston translational acceleration (see figure 15).

In conclusion the created engine model provides numerical results that are of practical interest in the tribodynamic study of engine performance. The numerical findings have been shown to agree well with experimental evidence and general well established analytical studies.

ACKNOWLEDGEMENTS

The authors would like to express their gratitude for the support of MDI UK Ltd and in particular to Mr.S. Gupta.

NOMENCLATURE

b	: Journal bearing width
c	: Bearing clearance
E	: Modulus of elasticity
h	: Lubricant film thickness
h_c	: Lower calorific value of fuel
h_t	: Instantaneous heat transfer coefficient
K_c	: Effective modulus of elasticity
$m\theta$: Mass fraction of burnt fuel
P	: Instantaneous cylinder pressure
Q	: Heat energy
R	: Radius of the journal
T	: Temperature
t	: Time
V	: Instantaneous cylinder volume
ν	: Poisson's ratio
ϵ	: Journal eccentricity
γ	: Ratio of specific heat for trapped gas
μ	: Lubricant viscosity

Subscripts

c	: belongs to the cylinder liner
p	: belongs to the piston
x_1, x_2	: in the x direction for body 1 and 2
y_1, y_2	: in the y direction for body 1 and 2

REFERENCES

- [1] Fantino, B., Godet, M. and Frene, J., "Dynamic behaviour of an elastic connecting-rod bearing- theoretical study", SAE/SP-539 Conf. Studies of Engine Bearings and Lubrication, Paper 83037, 1983, pp. 23-32.
- [2] Kryniski, K., "Jumping phenomenon in journal bearing", Trans. ASME, Rotating machinery and Vehicle Dynamics, DE-Vol. 35, 1991, pp. 169-173
- [3] Mehdigoli, H., Rahnejat, H and Gohar, R, "Vibration response of wavy surfaced disc in elastohydrodynamic rolling contact", Wear, Vol.139, 1990, pp. 1-15
- [4] Welbourn, D. B., "Fundemental knowledge of gear noise- A survey", Proc IMechE Vibrations in Transmissions Systems Conf., C117/79, 1979, pp. 9-14
- [5] Taylor, C. M., "Fluid film lubrication in automobile valve trains", Proc. Instn. Mech Engrs., Part J: J. Engng. Trib., Vol. 208, 1994, pp. 221-234
- [6] Bedewi, M. A., Dowson, D. and Taylor, C. M., "Elastrohydrodynamic lubrication of line contacts subjected to time depending loading with particular reference to roller bearings and cams and followers", Proc. 12th Leeds-Lyon Sympos. on Tribology- Mechanisms and Surface Stress, 1986, pp. 189-304, [Butterworths, Oxford]
- [7] Hanoka, M. and Fukumura, S., "A study of valve train noises and a method of cam design to reduce the noises", SAE Technical Paper 730247, 1973
- [8] Rahnejat, H and Gohar, R., "The vibrations of radial ball bearings", Proc Instn Mech Engrs, Part C: J. Mech. Engng. Sci., Vol. 199, No.C3, 1985, pp. 181-193
- [9] Aini, R., Rahnejat, H and Gohar, R., "An experimental investigation into bearing-induced spindle vibration", Proc Instn Mech Engrs, Part C: J. Mech. Engng. Sci., Vol. 209, 1985, pp. 107-114
- [10] Tuplin, W. A. , Torsional Vibration, Sir isaac Pitman and Sons Ltd, 1966
- [11] Draminsky, P., "Extended treatment of secondary resonance", Ship Building and Marine Engineering International, April 1988, Vol. 88, pp.180-186
- [12] Hestermann, D. C. and Stone, B. J., " The causes of torsional resonance in reciprocating engines and pumps at other than integer multiples of the fundemental excitation frequency", IMechE International Conference on Vibration and Rotating Machinery, C432/041, 1992, pp. 517-521
- [13] Bremer Jr., R. C., "A practical treatise on engine crankshaft torsional vibration control", SAE/SP-79/445, Proc. of West Coast Int. Meeting, 1979, Portland, USA, 1979, pp. 1-38
- [14] Dareing, D. W.,and Johnson, K. L., "Fluid film damping of rolling contact vibrations", J. Mech. Eng. Sci., 17(4), 1975, pp. 214-218
- [15] Zeischka, J., Mayer, L. S., Schersen, M. and Maessen, F., "Multi-body dynamics with deformable bodies applied to the flexible rotating crankshaft and the engine block", ASME 1994 Fall Technical Conference, Lafayette, Indiana, USA, October 2-5, 1994
- [16] Katano, H. Iwamoto, A. and Saitoh, T., "Dynamic behaviour analysis of internal combustion engine crankshafts under operating conditions", Proc. Instn. Mech. Engng., C430/049, 1991, pp. 205-209
- [17] Hestermann, D. C. and Stone, B. J., " Secondary inertia effects in the torsional vibration of reciprocating engines", Proc. Instn. Mech. Engng, 1994, 208(C1), pp.11-15

- [18] Song, X. G., Song, T. X., Xue, D. X. and Li, B. Z., "Progressive torsional-axial continued vibrations in crankshaft systems: A phenomenon of coupled vibration", Trans. ASME, Rotating Machinery and Vehicle Dynamics, 1991, pp. 319-323
- [19] Lacy, D. J., "Computers in analysis techniques for reciprocating engine design", IMechE C14/87, 1987, pp. 55-68
- [20] Kikuchi, K., "Analysis of unbalance vibration of a rotating shaft system with many bearings and discs", Bulletin of JSME, Vol. 13, No. 6, 1970
- [21] March, J. P. and Amphlett, S. A., "Studying low frequency vehicle phenomena using advanced modelling techniques, Part 1- Construction of driveline model", Int. Sympos. on Advanced Transportation Applications, SAE Pap. No. 94ME043, 1994
- [22] Wiebe, H., Brenverlauf und Kreisproze von Verbrennungsmotoren (Heat release and working cycle of IC engines), Berlin, Verlag Technik
- [23] Woschini, G.A., "A universally applicable equation for the instantaneous heat transfer coefficient in the internal combustion engine", SAE Pap. No. 850967, 1985
- [24] Noda, T., Yamamoto's, M., Ohmiya, Y., Kawamoto, J. and Nakada, M., "Analysis of oil consumption mechanism by measuring oil ring radial movement", SAE Paper 892104, 1989
- [25] Rahnejat, H., "Influence of vibration on the oil film in the concentrated contacts", PhD Thesis, Imperial College of Science and Technology, 1984.
- [26] Rahnejat, H., "Computational modelling of problems in contact dynamics", Engineering Analysis, Vol.2, No.4, 1985
- [27] Li, D.F., Rohde, S.M, and Ezzat, H.A., "An automotive piston lubrication model", ASLE Trans., Vol. 26, 2, pp.151-160
- [28] Dowson, D., Rudy, B.L. and Economou, P.N., "The elastohydrodynamic lubrication of piston rings", Proc. Royal Society A 386, 409-430, 1983
- [29] Moore, S.L. and Hamilton, G.M., "The piston ring at the top dead centre", Proc. Instn. Mech Engrs, Vol 194, pp. 373-381, 1980

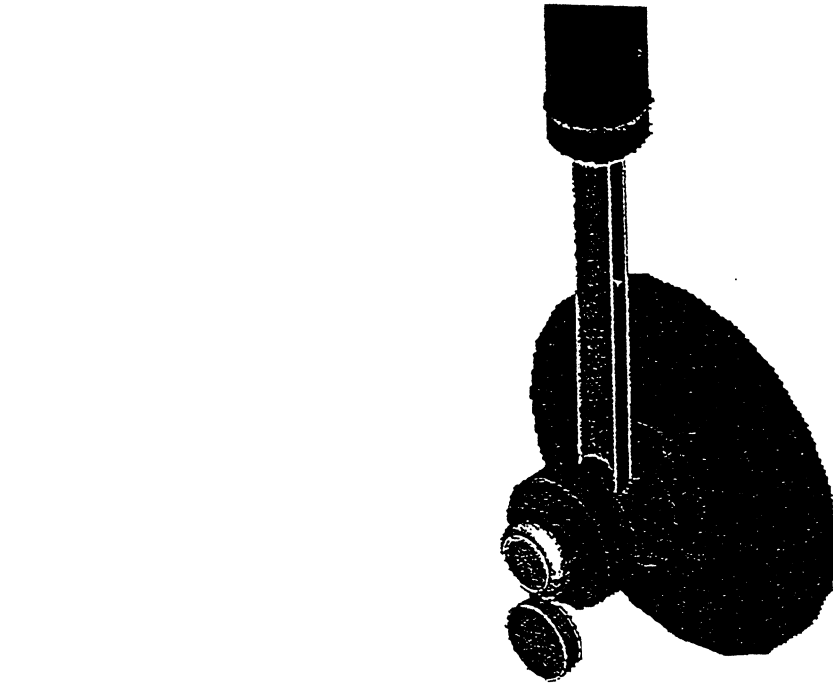


Figure 1

ADAMS/View model name: engine1
SFO9921: SFORCE/9921, FX, FY, FZ, FMAG

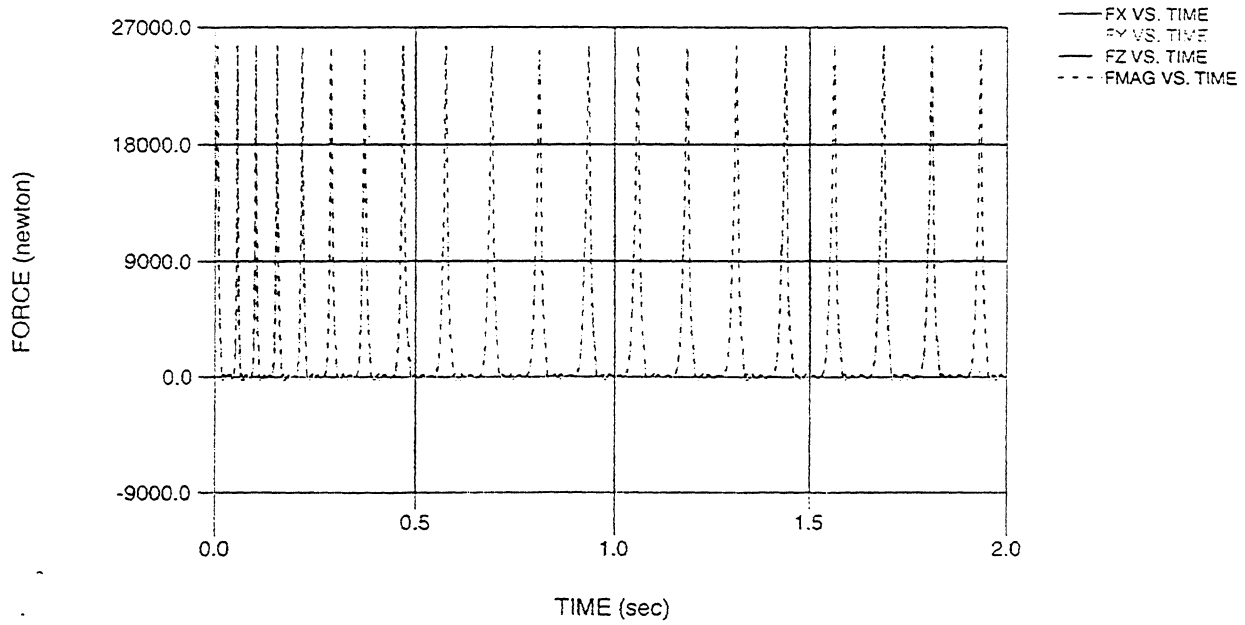


Figure 2

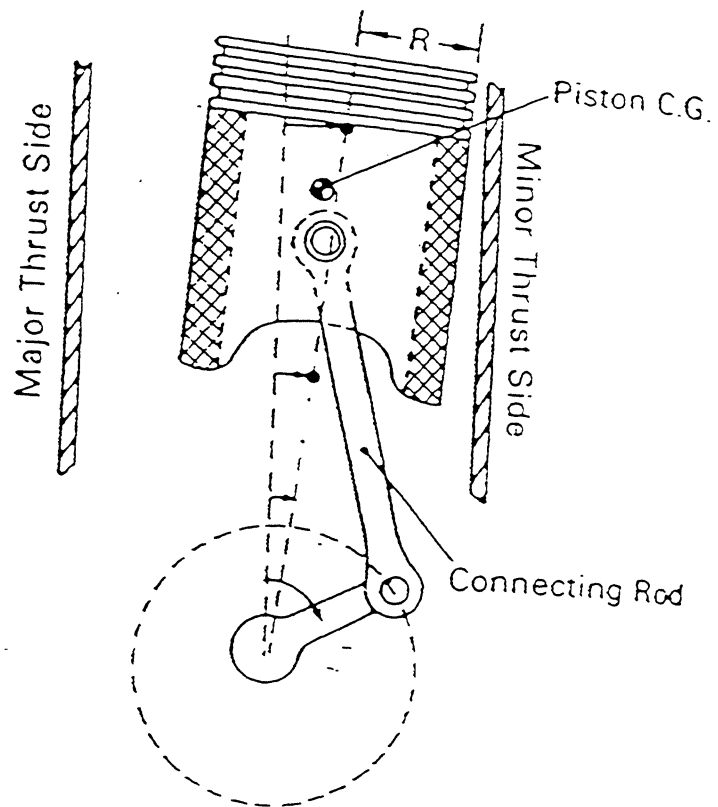


Figure 3

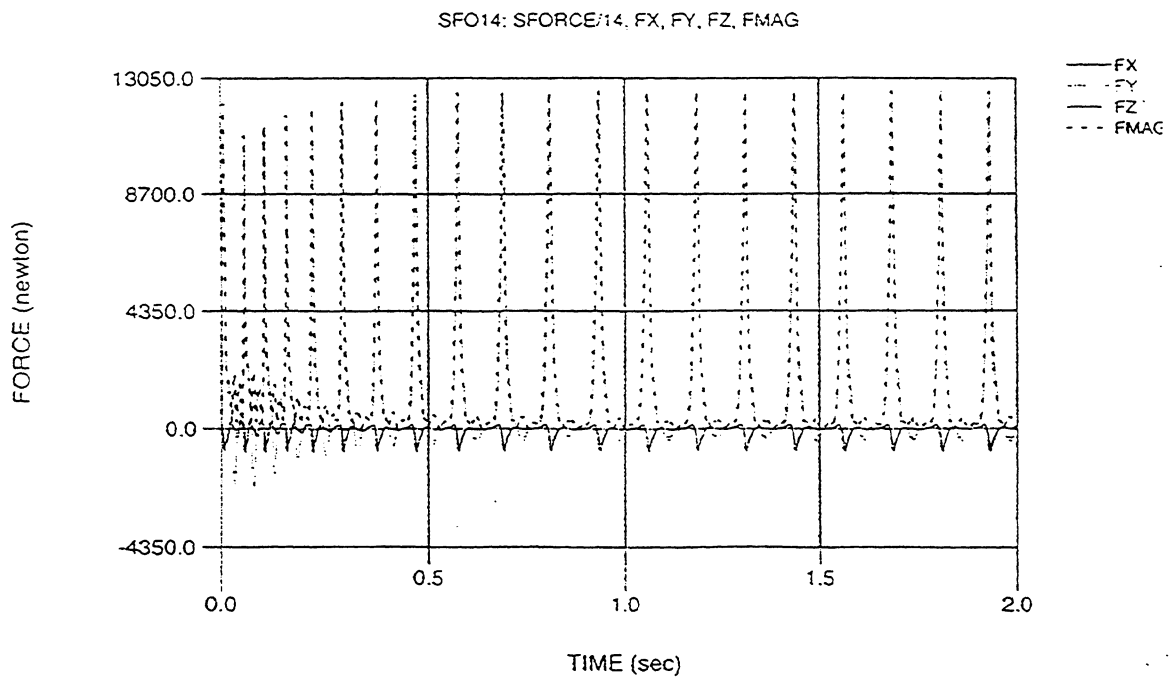


Figure4

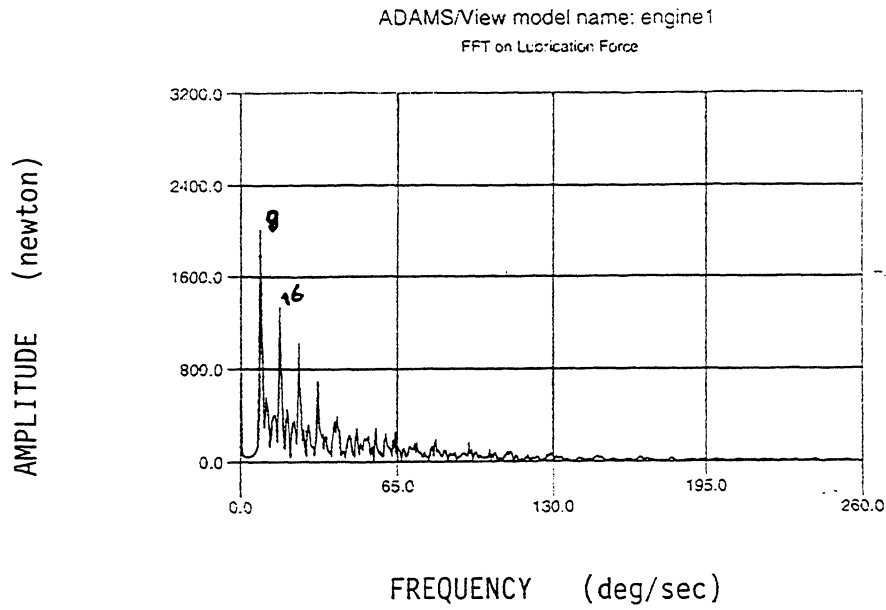


Figure 5

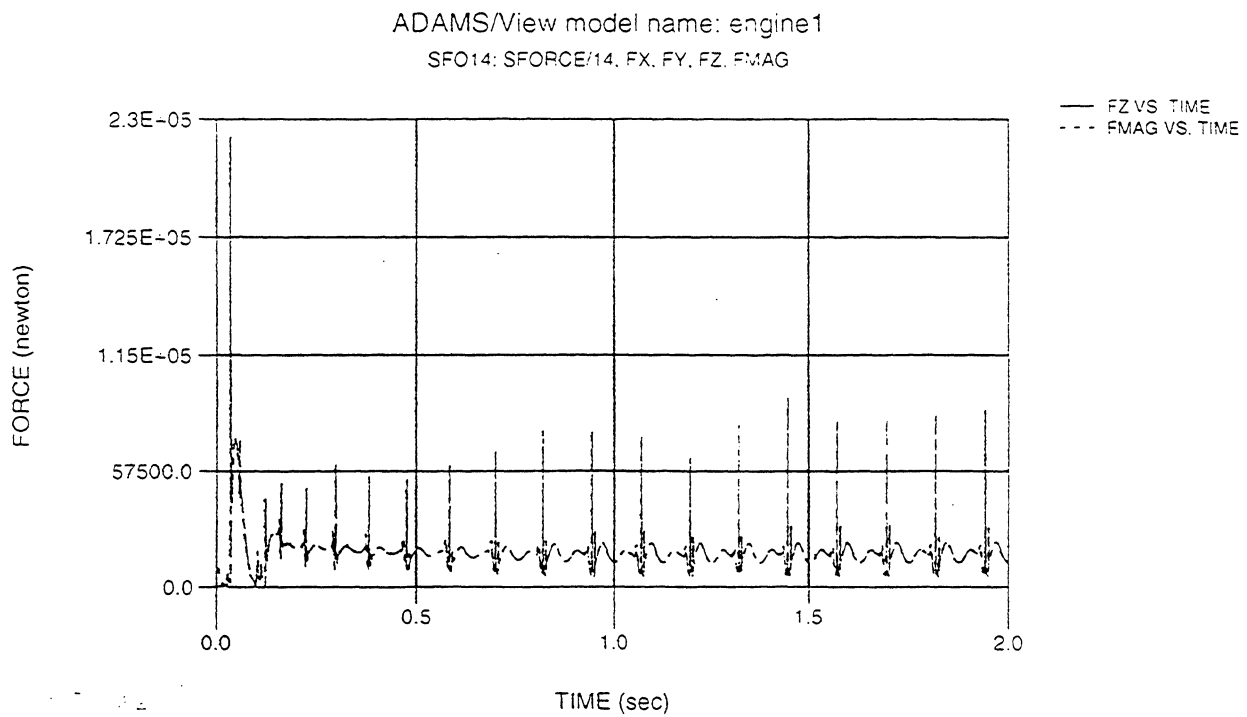


Figure 6

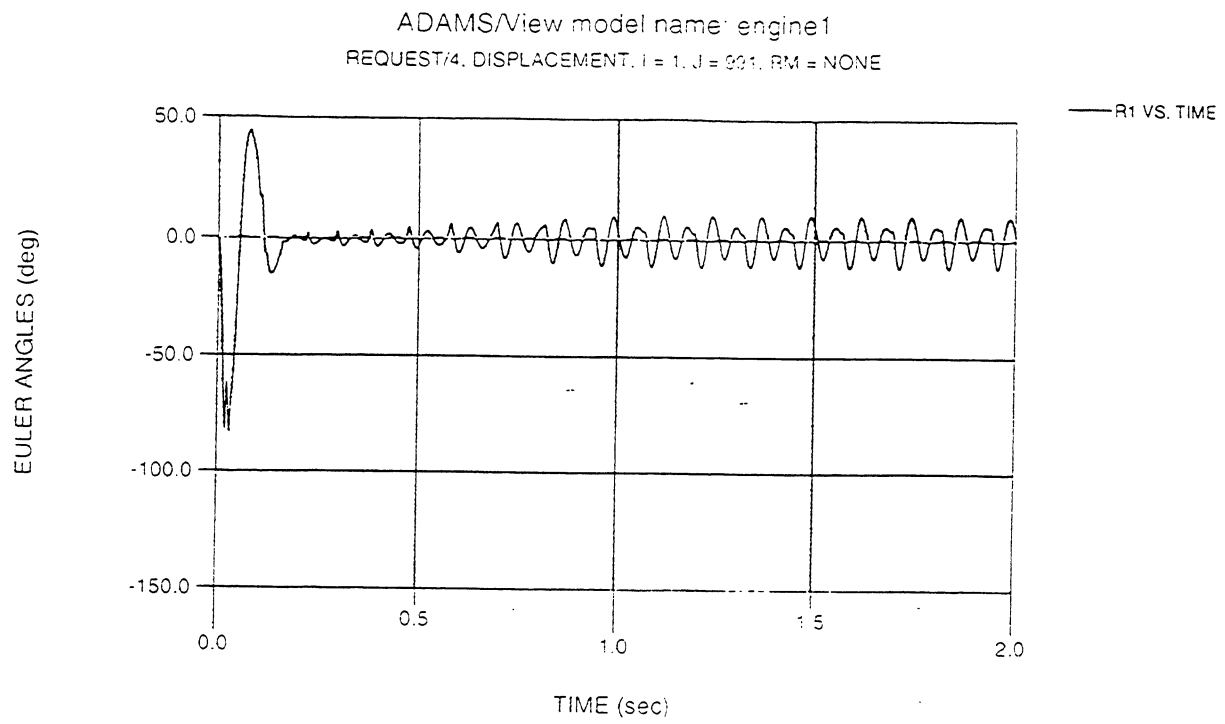


Figure 7

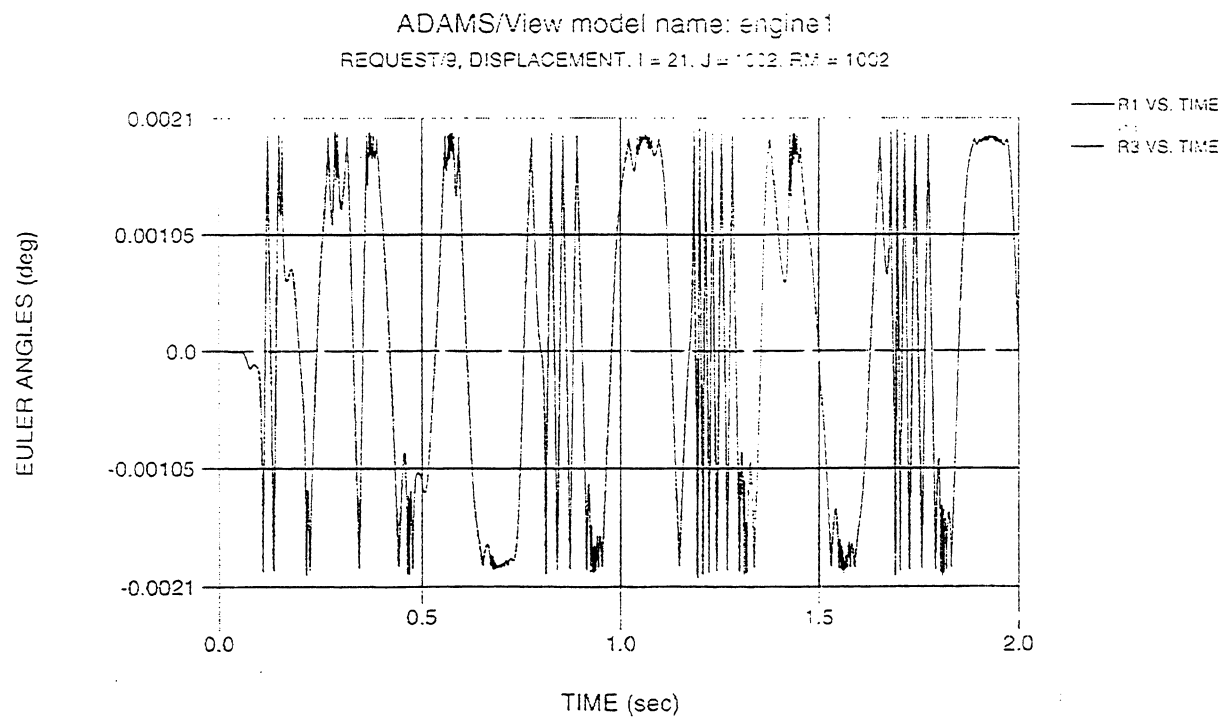


Figure 8

ADAMS/View model name: engine1
REQUEST:9, FORCE, I = 292, J = 9955, RM = NONE

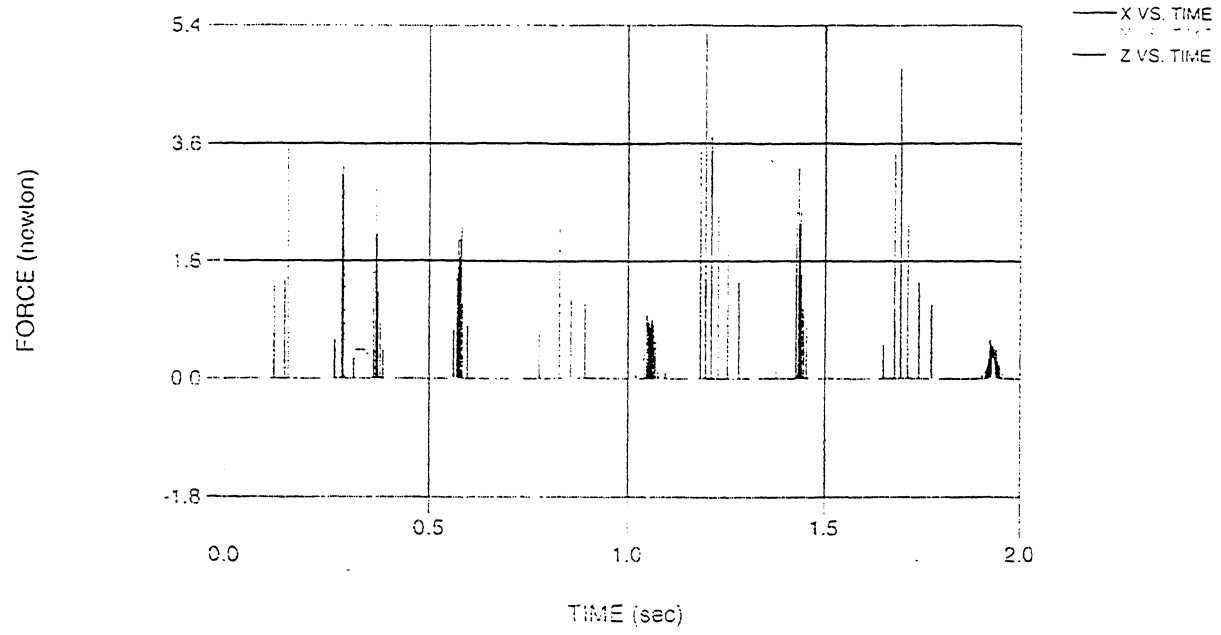


Figure 9

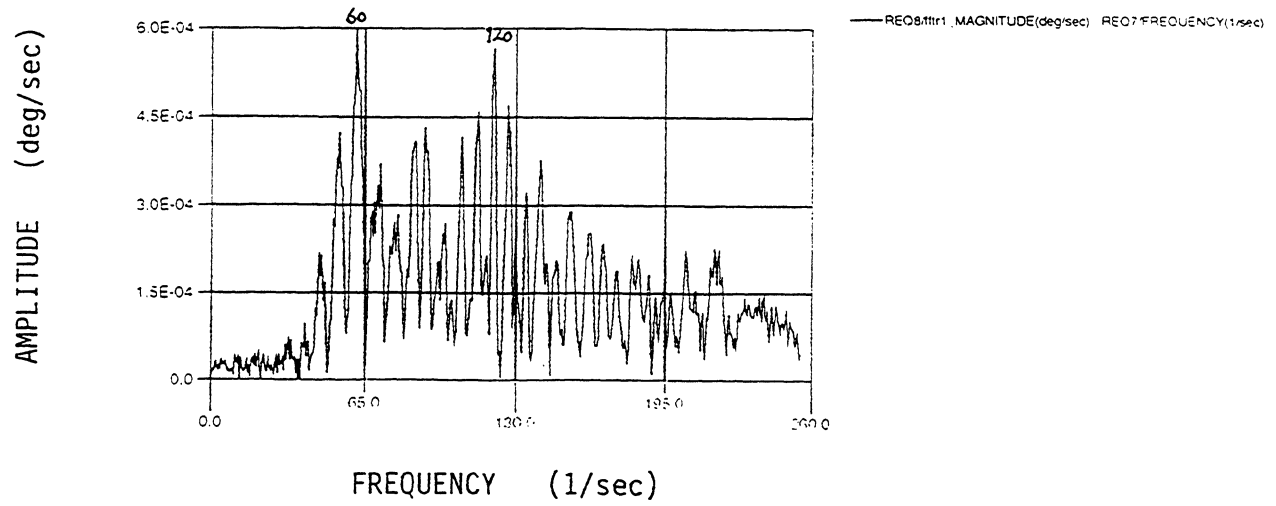


Figure 10

ADAMS/View model name: engine1
REQUEST/4, FORCE, I = 211 J = 2212, RM = NONE

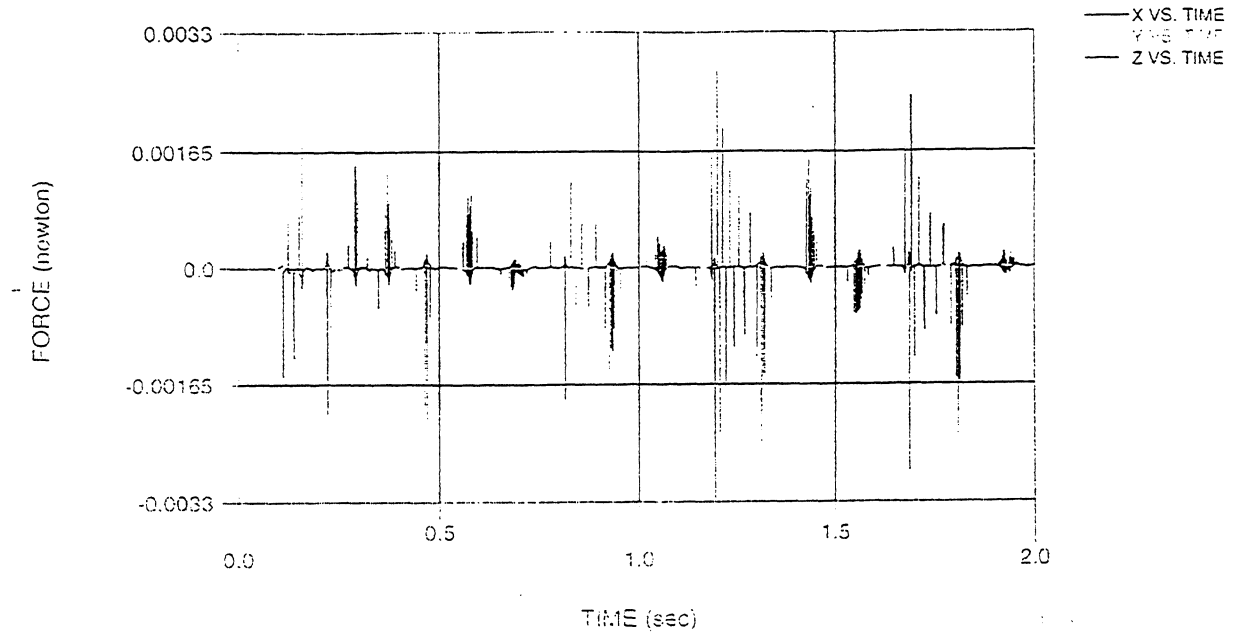
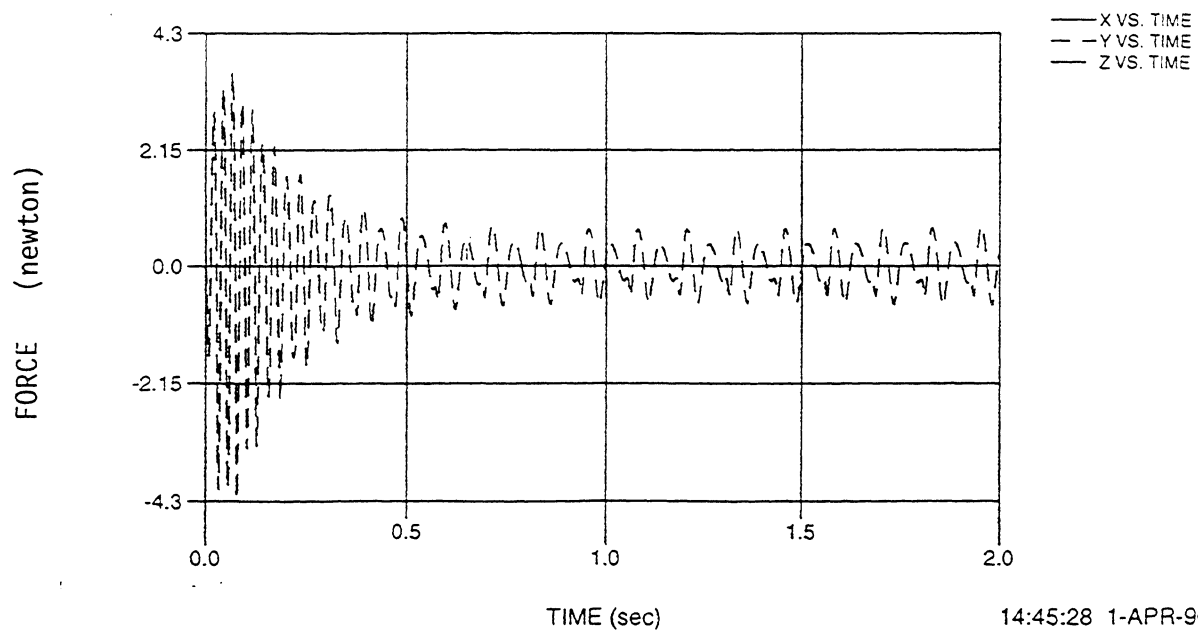


Figure 11

ADAMS/View model name: engine1
REQUEST/3, FORCE, I = 212, J = 221, RM = NONE



14:45:28 1-APR-96

Figure 12

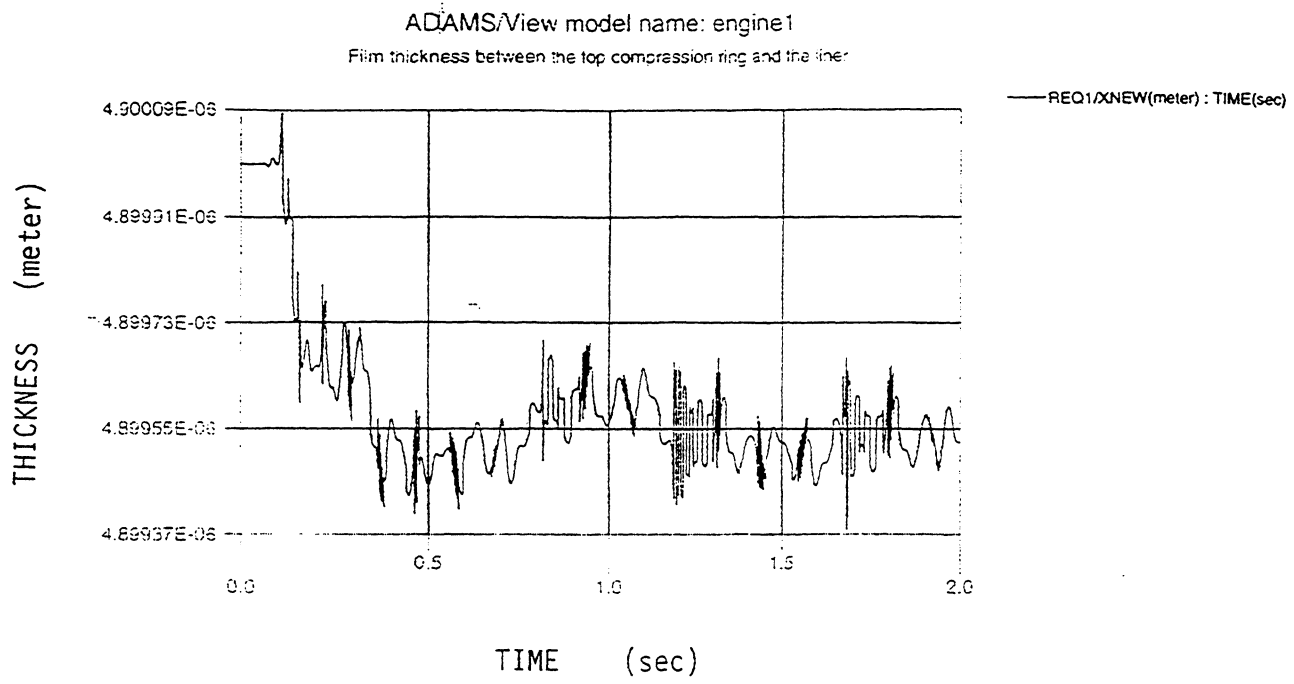


Figure 13

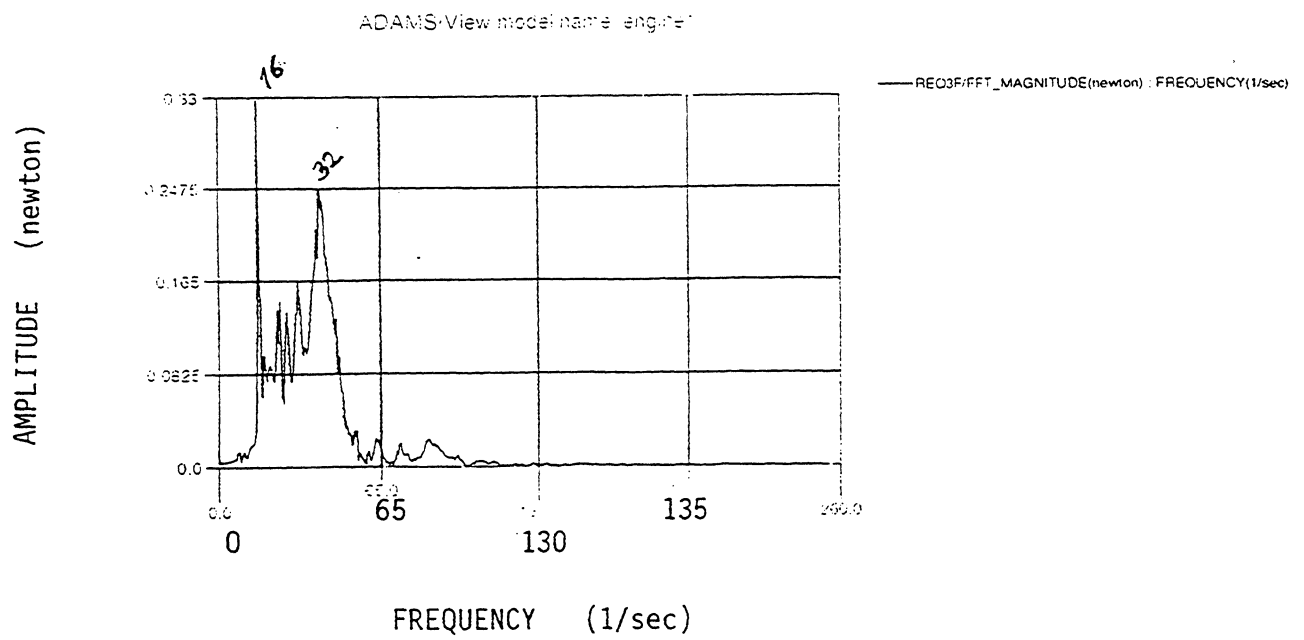


Figure 14

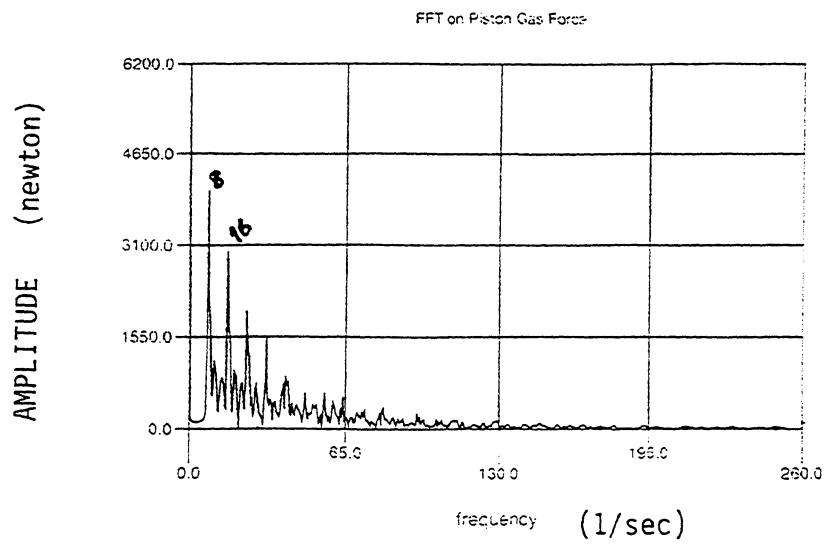


Figure 15

